

Observation of compensating Ga vacancies in highly Si-doped GaAs

T. Laine, K. Saarinen, J. Mäkinen, P. Hautojärvi, and C. Corbel*
Laboratory of Physics, Helsinki University of Technology, FIN-02150 Espoo, Finland

L. N. Pfeiffer and P. H. Citrin
Bell Laboratories, Lucent Technologies, Murray Hill, New Jersey 07974
 (Received 28 May 1996)

Positron annihilation experiments have been performed to study the type and concentration of compensating defects in highly Si-doped GaAs grown by molecular-beam epitaxy (MBE). The results show the presence of both Ga vacancies and negative ion defects, each of which act as acceptors in *n*-type GaAs. The concentrations of both types of defects increase strongly for Si concentrations exceeding $5 \times 10^{18} \text{ cm}^{-3}$. At $[\text{Si}] \geq 5 \times 10^{19} \text{ cm}^{-3}$, the concentrations of Ga vacancies and negative ions are comparable, and their sum represents a substantial fraction of the total concentration of Si itself. The results provide direct evidence that Ga vacancies play an important role in the electrical deactivation of highly Si-doped MBE-grown GaAs. [S0163-1829(96)51040-4]

Doping GaAs with Si efficiently yields free donor carriers so long as the doping level is low.¹ When concentrations of Si exceed $5 \times 10^{18} \text{ cm}^{-3}$, however, a strong deactivation is observed. This phenomenon is often attributed to autocompensation, whereby high Si concentrations lead to occupation of Si in both group-III and group-V lattice sites.² The Si_{As}^- acceptors compensate the Si_{Ga}^+ donors, resulting in a self-deactivation of electrical activity.

There is increasing evidence, however, that the autocompensation mechanism alone cannot account for the observed deactivation.³⁻⁷ For example, in GaAs doped with Si at $3 \times 10^{19} \text{ cm}^{-3}$, local vibration mode (LVM) spectra⁵ reveal three lines, which have been attributed to (i) Si acceptors, Si_{As}^- , (ii) neutral Si donor-acceptor pairs, $(\text{Si}_{\text{Ga}}-\text{Si}_{\text{As}})^0$, and (iii) Si atoms in a complex containing another point defect, (Si-X). The concentration of such (Si-X) complexes is inherently difficult to determine from LVM data.⁸ The identity of this point defect also remains unclear, although some arguments point to its being a Ga vacancy³⁻⁵ or an As vacancy.⁹

Positron annihilation spectroscopy can be used to study point defects in semiconductors, and in particular, vacancies. Positrons trapped at vacancy defects are experimentally observed as an increase in the positron lifetime and a narrowing of the momentum distribution of the annihilating electron-positron pairs.¹⁰ In addition to vacancies, positron measurements are sensitive to ion-type acceptors, since positrons are localized at the Rydberg state around the negative ions at low temperatures.¹¹

In this work, we use positron-annihilation measurements to study the compensating defects in highly Si-doped GaAs. Our data reveal vacancy-type acceptors, which we identify as Ga vacancy complexes, and ion-type acceptors, which we attribute to Si_{As}^- . The strong electrical deactivation observed in this system is shown to be largely explained by these two types of defects.

Highly Si-doped GaAs samples were grown by molecular-beam epitaxy (MBE) on (100)-oriented GaAs substrates at 900 K. The thickness of the Si-doped overlayer was $2 \mu\text{m}$. The Si-doping concentration in the four samples stud-

ied, determined⁷ by combining Hall measurements with x-ray-absorption, are (in units of 10^{18} cm^{-3}) approximately 2, 3, 9, and 50. Following Ref. 7, the samples are referred to here as "low" (*L*), "medium" (*M*), "high" (*H*), and "very high" (*VH*), respectively. The strong electrical deactivation was seen only in the *H* and *VH* samples. Si *K* near-edge x-ray-absorption fine-structure (NEXAFS) measurements⁷ were used to determine upper limits for the Si_{As} concentrations of about $1 \times 10^{18} \text{ cm}^{-3}$ for the *H* sample and $2 \times 10^{19} \text{ cm}^{-3}$ for the *VH* sample. These concentrations, corresponding to only 12% and 38% of the total Si, respectively, provide direct evidence that autocompensation cannot fully explain the observed electrical inactivity.

The epitaxially grown Si-doped GaAs layers of Si were measured using the low-energy positron beam technique.¹² For reference, a *p*-type Be-doped ($4 \times 10^{16} \text{ cm}^{-3}$) GaAs layer grown by MBE was also studied. The 511-keV annihilation line was measured at 20-keV incident positron energy, which corresponds to a mean positron stopping depth in GaAs of $0.9 \mu\text{m}$. At this energy, the contributions of annihilation events at the surface and in the substrate are negligible. Doppler broadening of the 511-keV radiation gives information about the momentum distribution of annihilating electrons. The momentum distribution is usually described in terms of the valence and core annihilation parameters *S* and *W*. The *S* parameter, defined as the relative amount of annihilation events over the energy range $511 \pm 0.95 \text{ keV}$ around the peak centroid, represents the electron-positron pairs with longitudinal momentum component $p_L/m_0c \leq 3.7 \times 10^{-3}$ that arise mainly from annihilations with valence electrons (m_0 is the electron mass and *c* is the speed of light). The *W* parameter, defined as the relative number of events in the momentum range $p_L/m_0c = (15-20) \times 10^{-3}$, represents annihilations involving core electrons of atoms surrounding a vacancy. The core electron momentum distribution at a broader p_L range of $(10-40) \times 10^{-3}$ can be studied in detail with coincidence measurements of the two 511-keV photons.¹³ This technique is applied here to identify the sublattice of the vacancy defects.

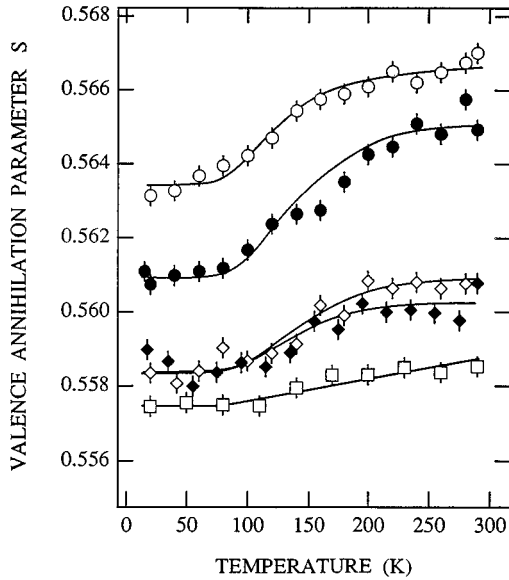


FIG. 1. The valence annihilation parameter S was measured in Be-doped GaAs (\square), and in Si-doped GaAs samples with $[\text{Si}] \approx 1 \times 10^{18} \text{ cm}^{-3}$ (\blacklozenge), $3 \times 10^{18} \text{ cm}^{-3}$ (\diamond), $9 \times 10^{18} \text{ cm}^{-3}$ (\bullet), and $5 \times 10^{19} \text{ cm}^{-3}$ (\circ), all as a function of temperature between 20 and 300 K.

The valence annihilation parameter S for the Be-doped GaAs layer and the four Si-doped GaAs layers is plotted against temperature in Fig. 1. In Be-doped GaAs it is seen to be nearly temperature independent, which is typical for free positron annihilation in the bulk. In all of the Si-doped samples, the S parameter is clearly larger and it is temperature dependent. Focusing on the magnitude of S , we see that the increase of positron trapping at vacancies with Si concentration is particularly strong when it exceeds $5 \times 10^{18} \text{ cm}^{-3}$, behavior paralleling that of the observed⁷ electrical deactivation. To see if there are any illumination effects on these vacancy defects, which would indicate metastability related to DX centers,¹⁴ the samples were illuminated for several hours at 20 K with 1.32-eV photons. The S parameter remained unchanged during and after the illuminations.

Coincidence measurements of core electron momentum distributions were obtained from the Be-doped and VH Si-doped GaAs samples at room temperature. The high-momentum parts of the Doppler curves, area normalized, are plotted as filled diamonds and circles in Fig. 2. The momentum distribution $\rho(p)$ of Be-doped GaAs is characteristic of free positrons in a GaAs lattice and has a noticeably higher intensity than that in the VH sample. This result clearly shows the effect of positrons trapped at vacancies in the VH sample: at such defects containing more open volume, the overlap between positrons and core electrons of the surrounding atoms is reduced.

The shape of the distribution in the VH sample is also different from that in the GaAs lattice. Although the differences are small, the momentum distribution $\rho(p)$ in the VH sample is clearly broader than in the Be-doped reference sample. An exponential fit $\rho(p) \propto e^{-\lambda p}$ in the momentum range $p = (15-35) \times 10^{-3} m_0 c$ yields a coefficient $\lambda = 0.257(2) \times 10^3 / m_0 c$ in the Be-doped GaAs, whereas a

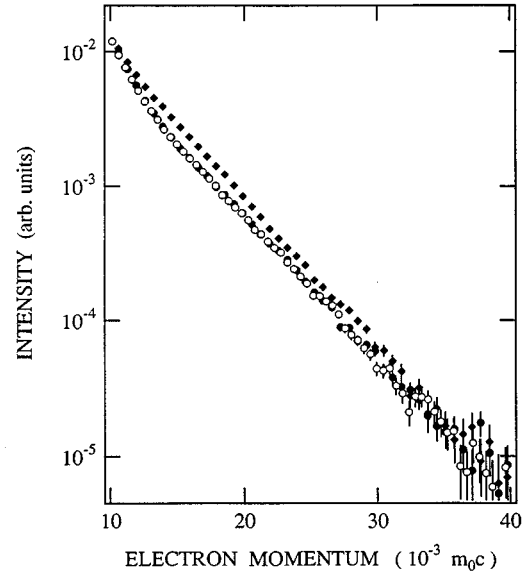


FIG. 2. The core electron momentum distribution in Be-doped GaAs (\blacklozenge), in electron-irradiated semi-insulating GaAs (\circ) (from Ref. 15), and in GaAs ($[\text{Si}] = 5 \times 10^{19} \text{ cm}^{-3}$) (\bullet).

clearly smaller coefficient of $\lambda = 0.246(2) \times 10^3 / m_0 c$ is obtained in the VH sample.

The differences in the shapes of the momentum distributions are interpreted in the following way. For free positrons in GaAs, the dominant contribution to the measured core electron momentum distribution comes from the $3d$ electrons of Ga atoms ($Z=31$). The $3d$ electrons of As atoms ($Z=33$) are more tightly bound, leading to a broader momentum distribution and a reduced overlap with the positrons.¹³ The broader distribution in the VH sample therefore indicates that the relative amount of positron annihilation with the As core electrons is larger at the vacancy than in the GaAs lattice. This implies that the vacancy in the VH sample is surrounded by As atoms and is thus associated with the Ga sublattice.

There is firmer evidence for this assignment. Positron trapping at Ga vacancies has been previously observed in electron-irradiated GaAs.¹⁵ The core electron momentum distribution associated with irradiation-induced V_{Ga} has been plotted with open circles in Fig. 2. Its shape is essentially identical to that measured in the VH sample. It further yields the same coefficient $\lambda = 0.248(2) \times 10^3 / m_0 c$ in an exponential fit of $\rho(p) \propto e^{-\lambda p}$ at $p = (15-35) \times 10^{-3} m_0 c$. Denoting the core annihilation parameter in the bulk lattice by W_B , the relative parameter W/W_B is 0.71(1) for the VH sample and 0.73(1) for the irradiation-induced sample. The striking similarity in both intensity and shape leads us to conclude that the vacancy observed in the VH sample is a Ga vacancy. The present data alone do not, however, tell us whether the Ga vacancy is isolated, V_{Ga}^{3-} or associated with a Si donor, $(\text{Si}_{\text{Ga}}-V_{\text{Ga}})^{2-}$, because the Si atom on a second-neighbor site does not contribute much to the core annihilations.

Chadi has recently calculated that, under equilibrium conditions, a relaxed $V_{\text{As}}\text{-Si}_{\text{Ga}}$ pair is an abundant acceptor in

Si-doped GaAs and is thus a potential compensating center.⁹ Our results indicate that (nonequilibrium) MBE growth of Si-doped GaAs generates vacancies in the Ga sublattice rather than the As sublattice. Earlier, we have identified As vacancies in liquid-encapsulated Czochralski grown *n*-doped GaAs crystals.¹⁶ The core momentum distribution for the As vacancy is more narrow at $(20\text{--}40)\times 10^{-3}m_0c$ than that obtained for the Ga vacancy in the *VH* or electron irradiated samples.¹⁷

The temperature dependence of the *S* parameter in Fig. 1 is similar in all four Si-doped samples. The *S* parameter is first constant at 10–100 K, then increases from 100 to 200 K, and finally reaches a plateau around 300 K. The plateau levels were confirmed by experiments between 300–600 K (not shown). The *S* parameter decreases in all layers when *T* is lowered to 20 K, a trend opposite to that observed¹⁵ for positron trapping at negative Ga vacancies at low *T*. This indicates that another defect must be competing with the Ga vacancy for trapping positrons in Si-doped GaAs at 20 K.

We attribute these competing defects to negative ions, which have no open volume associated with them.^{11,15} The negative ions bind positrons to shallow (<0.1 eV) Rydberg states,¹⁸ whose annihilation characteristics are similar to those in the lattice due to the weak positron localization. Below 100 K, all positrons are trapped at either Ga vacancies or negative ions. The increase in the *S* parameter above 100 K indicates that positrons are partially detrapped from the negative ions, and a larger fraction of them annihilates at the Ga vacancies. When the detrapping is complete above 200 K, only Ga vacancies trap positrons, and the *S* parameter reaches a plateau with a magnitude that depends on $[V_{\text{Ga}}]$.

To quantify the concentration of vacancies and ions, we have analyzed the temperature dependence of the *S* parameter using a positron trapping model.¹⁵ The positron trapping rate at the vacancies, κ_v , is proportional to the vacancy concentration c_v by $\kappa_v = \mu_v c_v$. The positron trapping coefficient μ_v is temperature dependent, and a value of $1.4 \times 10^{15} \text{ s}^{-1}$ at 300 K is used.^{15,19–21} The positron trapping rate at the negative ions is similarly modeled by $\kappa_{\text{ion}} = \mu_{\text{ion}} c_{\text{ion}}$, where the corresponding trapping coefficient¹⁸ $\mu_{\text{ion}} \propto T^{-1/2}$. The positron detrapping rate from the ions is $\delta \propto \mu_{\text{ion}}(kT)^{3/2} \exp(-E_{b,\text{ion}}/kT)$, with $E_{b,\text{ion}}$ being the positron binding energy at the ion.²² Denoting the valence annihilation parameter in the bulk by S_B , we get the *S* parameter for the negative ions, $S_{\text{ion}} = S_B$, and for the Ga vacancy we use $S_{v(\text{Ga})} = 1.015 S_B$.²³ The four adjustable parameters used in fitting the data are then c_v , c_{ion} , μ_{ion} , and $E_{b,\text{ion}}$. Details of this type of analysis have been given elsewhere.^{15,20}

The solid lines in Fig. 1 are the fits to the measured *S* parameters. Initial fits with all adjustable parameters left unconstrained consistently gave a positron binding energy of $E_{b,\text{ion}} = 40 \pm 10$ meV. Subsequent refinements with $E_{b,\text{ion}}$ fixed at 40 meV lead to a positron trapping coefficient of $\mu_{\text{ion}} = (4.5 \pm 1.0) \times 10^{16} T^{-1/2} \text{ s}^{-1}$ (*T* is in degrees of Kelvin). Values of the remaining two parameters, namely, the concentration of vacancies c_v and negative ions c_{ion} are shown as a function of Si concentration in Fig. 3.²⁴

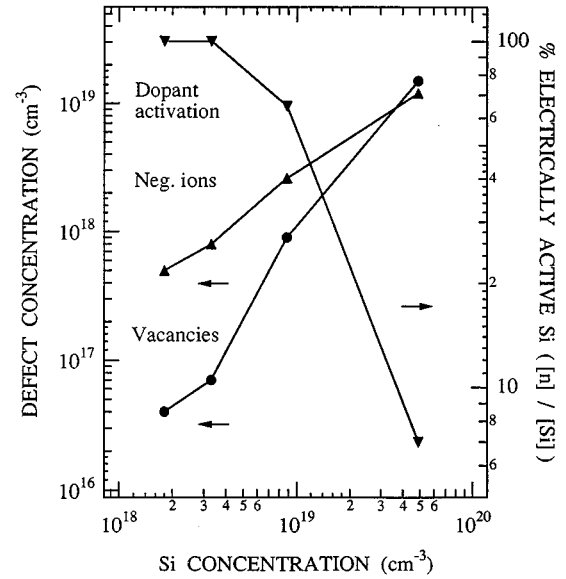


FIG. 3. The dopant activation, expressed as the ratio of free carrier and Si concentrations (\blacktriangledown), the concentration of negative ions (\blacktriangle), and the concentration of Ga vacancies (\bullet) all as a function of Si concentration in four Si-doped GaAs samples.

Two results are immediately apparent. First, in the overall trend of values for c_v and c_{ion} there is a marked increase in both as $[\text{Si}]$ increases, particularly going from the *L* and *M* samples to the *H* and *VH* samples. Second, the magnitudes of both c_v and c_{ion} relative to $[\text{Si}]$ in the respective samples change dramatically: in the *L* and *M* samples, the combined sum of these defect concentrations is $<25\%$ of the Si doping concentration, while in the *H* and *VH* samples this fraction is $>50\%$ $[\text{Si}]$.

The effect of these defects becomes apparent when we plot as a function of $[\text{Si}]$ the measured⁷ electrical activity of Si, defined as the ratio of free carrier to Si concentrations, $[n]/[\text{Si}]$ (see Fig. 3). It is clear that the sharp decrease in activity correlates strongly with the summed concentrations of negative ions and vacancies in the *H* and *VH* samples. Both types of defects compensate free carriers, and both must be important in describing the electrical deactivation in highly Si-doped GaAs.

To identify the nature of these defects and determine the possible importance of other defects as well, we must combine the results of the present work with those obtained in previous studies. Thus, as already stated, our positron data alone cannot distinguish between the singly negative ion Si_{As}^- and an intrinsic defect like the doubly negative Ga antisite, $\text{Ga}_{\text{As}}^{2-}$,^{2–15} nor can they distinguish between a Ga vacancy complex, such as $(\text{Si}_{\text{Ga}}-\text{V}_{\text{Ga}})^{2-}$ and an isolated Ga vacancy, $\text{V}_{\text{Ga}}^{3-}$. However, by combining our knowledge of (a) the existence of Si_{As}^- monomers, $(\text{Si}_{\text{Ga}}-\text{Si}_{\text{As}})^0$ dimers, Si_n clusters, and $(\text{Si}_{\text{Ga}}-\text{X})$ complexes from LVM (Ref. 5) and x-ray absorption (NEXAFS) and EXAFS⁷ measurements, (b) the upper limit concentrations of $[\text{Si}_{\text{As}}^-]$ determined in Ref. 7, and (c) the distributions (albeit under equilibrium conditions) of defect species calculated in Ref. 6, with (d) the constraints imposed by charge and mass conservation, and (e) our present findings, we arrive at the following conclusions. In MBE-grown highly Si-doped GaAs (i.e.,

$[\text{Si}] > 5 \times 10^{18} \text{ cm}^{-3}$), the most likely assignment of the negative ion species is Si_{As}^- , and of the Ga vacancy is $(\text{Si}_{\text{Ga}}-\text{V}_{\text{Ga}})^{2-}$. These two defects are dominant for their generic type. Together, they account for a large part of the observed compensation of heavily Si-doped GaAs. The con-

centrations of other electrically inactive defects, e.g., $[\text{Si}_{\text{Ga}}-\text{Si}_{\text{As}}]$ dimers and $[\text{Si}_n]$ clusters, or of more strongly compensating defects, e.g., $[\text{Ga}_{\text{As}}^{2-}]$ antisites and isolated Ga vacancies $[\text{V}_{\text{Ga}}^{3-}]$, are much less important in these samples.

-
- *Permanent address: Institut National des Sciences et Techniques Nucléaires, Centre d'Etudes de Saclay, 91191 Gif-sur-Yvette Cedex, France.
- ¹Y. G. Chai, R. Chow, and C. E. C. Wood, *Appl. Phys. Lett.* **39**, 800 (1981).
- ²For a recent review, see E. F. Schubert, *Doping in III-V Semiconductors* (Cambridge University, Cambridge, 1993).
- ³S. Chichibu, A. Iwai, Y. Nakahara, S. Matsumoto, H. Higuchi, L. Wei, and S. Tanigawa, *J. Appl. Phys.* **73**, 3880 (1993).
- ⁴J. L. Lee, L. Wei, S. Tanigawa, and M. Kawabe, *J. Appl. Phys.* **68**, 5571 (1990).
- ⁵J. Maguire, R. Murray, R. C. Newman, R. B. Beall, and J. J. Harris, *Appl. Phys. Lett.* **50**, 516 (1987).
- ⁶J. E. Northrup and S. B. Zhang, *Phys. Rev. B* **47**, 6791 (1993); S. B. Zhang and J. E. Northrup, *Phys. Rev. Lett.* **67**, 2339 (1991).
- ⁷S. Schuppler, D. L. Adler, L. N. Pfeiffer, K. W. West, E. E. Chaban, and P. H. Citrin, *Appl. Phys. Lett.* **63**, 2357 (1993); *Phys. Rev. B* **51**, 10 527 (1995).
- ⁸R. Murray, R. C. Newman, M. J. L. Sangster, R. B. Beall, J. J. Harris, P. J. Wright, J. Wagner, and M. Ramsteiner, *J. Appl. Phys.* **66**, 2589 (1989).
- ⁹J. Chadi (private communication).
- ¹⁰*Positron Spectroscopy of Solids*, edited by A. Dupasquier and A. P. Mills (IOS Press, Amsterdam, 1995).
- ¹¹K. Saarinen, P. Hautojärvi, A. Vehanen, R. Krause, and G. Dlubek, *Phys. Rev. B* **39**, 5287 (1989).
- ¹²J. Lahtinen, A. Vehanen, H. Huomo, J. Mäkinen, P. A. Huttunen, K. Rytölä, M. Bentson, and P. Hautojärvi, *Nucl. Instrum. Methods Phys. Res. B* **17**, 73 (1986).
- ¹³M. Alatalo, H. Kauppinen, K. Saarinen, M. J. Puska, J. Mäkinen, P. Hautojärvi, and R. M. Nieminen, *Phys. Rev. B* **51**, 4176 (1995).
- ¹⁴J. Mäkinen, T. Laine, K. Saarinen, P. Hautojärvi, C. Corbel, V. M. Airaksinen, and P. Gibart, *Phys. Rev. Lett.* **71**, 3154 (1993).
- ¹⁵C. Corbel, F. Pierre, K. Saarinen, P. Hautojärvi, and P. Moser, *Phys. Rev. B* **45**, 3386 (1992).
- ¹⁶K. Saarinen, P. Hautojärvi, P. Lanki, and C. Corbel, *Phys. Rev. B* **44**, 10 585 (1991); C. Corbel, M. Stucky, P. Hautojärvi, K. Saarinen, and P. Moser, *ibid.* **38**, 8192 (1988).
- ¹⁷S. Kuisma, K. Saarinen, and P. Hautojärvi (unpublished).
- ¹⁸M. J. Puska, C. Corbel, and R. M. Nieminen, *Phys. Rev. B* **41**, 9980 (1990).
- ¹⁹K. Saarinen, S. Kuisma, J. Mäkinen, P. Hautojärvi, M. Törnqvist, and C. Corbel, *Phys. Rev. B* **51**, 14 152 (1995).
- ²⁰K. Saarinen, A. P. Seitsonen, P. Hautojärvi, and C. Corbel, *Phys. Rev. B* **52**, 10 932 (1995).
- ²¹C. LeBerre, C. Corbel, K. Saarinen, S. Kuisma, P. Hautojärvi, and R. Fornari, *Phys. Rev. B* **52**, 8112 (1995).
- ²²M. Manninen and R. M. Nieminen, *Appl. Phys. A* **26**, 93 (1981).
- ²³K. Saarinen, S. Kuisma, P. Hautojärvi, C. Corbel, and C. LeBerre, *Phys. Rev. B* **49**, 8005 (1994).
- ²⁴Note that our analysis gives only lower limits of c_v and c_{ion} in the *VH* sample, because the measured *S* parameter at 300 K is very close to the defect parameter $S_{v(\text{Ga})}$.